MOLECULAR DYNAMICS SIMULATIONS OF PHONON TRANSPORT IN SINGLE-WALLED CARBON NANOTUBES

°Junichiro SHIOMI and Shigeo MARUYAMA
Department of Mechanical Engineering, The University of Tokyo, Tokyo 113-8656, Japan
Corresponding author: Junichiro Shiomi, E-mail: shiomi@photon.t.u-tokyo.ac.jp

We report a non-equilibrium molecular dynamics (MD) study on heat conduction of finite-length single-walled carbon nanotubes (SWNTs). The length-dependence of the thermal conductivity is quantified for a range of nanotube-lengths (25 nm<L<3.2 μm) at room temperature using two different temperature control techniques. The trend of length effect indicates a gradual transition from nearly pure ballistic phonon transport to diffusive-ballistic phonon transport. The limit of ballistic transport was found to exceed 3.2 μm. Thermal conductivity is diameter-independent for short SWNTs (L< 100 nm) due to a significant contribution of ballistic transport of optical phonons in heat conduction.

1. Introduction

The ever-expanding expectations for single-walled carbon nanotubes (SWNTs) include applications for various electrical and thermal devices due to their unique electrical and thermal properties [1]. SWNTs are expected to possess high thermal conductivity due to their strong carbon bonds and the quasi-one-dimensional structure [2]. On considering the actual applications, one of the essential tasks is to characterize the thermal properties not only for thermal devices but also for electrical devices since they may limit the affordable amount of electrical current through the system.

With recent advances in SWNT synthesis and MEMS techniques, thermal conductivity (or conductance) measurements have been reported for a few micrometers long individual suspended SWNTs [3, 4], where the values were around a few thousands W/mK, similar to those of multi-walled carbon nanotubes [5, 6]. However, as the thermal measurements of nanomaterial are technically challenging, there are certainly rooms for uncertainties for instance related to contact resistances between thermal reservoirs and an SWNT. Therefore, the demands for reliable theories and numerical simulations are greater than ever not only for validations of the experimental results but also for probing the detail characteristics of heat conduction that are not accessible in experiments.

One of the important thermal characteristics in practical situations that are difficult to probe with experiments is the geometry dependence of the thermal conductivity. Thermal conductivity of SWNTs exhibits a distinct length effect. In general, the size-dependence of the thermal conductivity appears when the system characteristic length is smaller or comparable to the phonon mean free path [7]. For SWNTs, due to the expected long phonon mean free path, the regime of the length-effect stretches beyond the realistic length in many applications. The length effect was demonstrated using MD simulations [8, 9] and the power-law dependence was discussed in analog to the convectional one-dimensional models [10]. Recently the relation of exponents to the diffusive-ballistic phonon transport is discussed using kinetic approach [11] and an energy transmission model [12].

In this study, we aim to investigate the phonon transport in SWNTs for a range of SWNT lengths (25 nm<L<3.2 μm) by performing non-equilibrium MD simulations.

2. Molecular dynamics simulations

In MD simulations presented in the current report, the carbon-carbon interactions were modeled using the Brenner potential [13] in the simplified form [14] where the total potential energy of the system is expressed as,

$$E = \sum_i \sum_{j(i<j)} \left[V_R(r_{ij}) - B^*_{ij} V_A(r_{ij}) \right]. \quad (1)$$

Here, $V_R(r)$ and $V_A(r)$ are repulsive and attractive force terms which take the Morse type form with a certain cut-off function. B^*_{ij} represents the effect of the bonding order parameters. As for the potential parameters, we employ the set that was shown to reproduce the force constant better (Table 2 in [13]). The velocity Verlet method was adopted to integrate the equation of motion with the time step of 0.5 fs.

The use of classical approach is encouraged by the

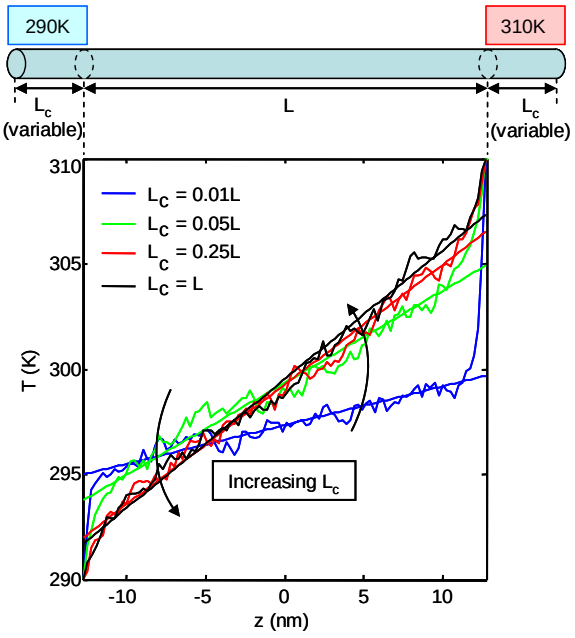

Figure 1 Influence of L_c on the temperature jump between the temperature controlled part and the rest of the SWNT. Nose-Hoover thermostats are used to impose the temperature gradient.

expected dominant contribution on the heat conduction from phonons compared with that from electrons [15]. Not only the electric thermal conductance for semi-conducting SWNTs which is expected to be negligible, but also the electric contribution of metallic SWNTs has been calculated to be minor (~10%) at room temperature [16].

3. Results and Discussions

3.1 Thermal conductivity measurements

Thermal conductivity λ of SWNTs was measured following the methodology similar to that of the previous reports [8, 9] but for much longer SWNTs. After reaching the isothermal state at 300 K with the auxiliary velocity scaling control, the thermostat layers on both ends of the SWNT were activated to apply a temperature difference of 20 K to achieve a quasi-stationary temperature gradient. By calculating the heat flux along the tube from the energy budgets of the thermostats, λ can be calculated through the Fourier's law $q = -\lambda dT/dz$. The cross-sectional area A of a nanotube was defined as $A = 2\sqrt{3}(d/2 + b/2)^2$, the area of a hexagon dividing a bundle of SWNTs, where b=0.34 nm is van der Waals thickness. The usage of thermal conductivity to express the heat conduction of the current system is arguable since the length dependence makes the thermal conductivity not a unique physical property anymore. Furthermore, the definition of the area of an isolated SWNT is rather trivial. Although simply expressing the heat conduction with thermal conductance may be more suitable, here we use thermal conductivity for the sake of comparison with previous studies.

As for the thermostats, in addition to the phantom technique (Langevin method) used in the earlier works [9, 10], we adopt a straightforward application of Nose-Hoover (NH) thermostats [17, 18]. On carrying out non-equilibrium MD simulations by applying thermostats to the tube-ends with length L_c, the interface between the temperature-controlled part and the rest of the SWNT typical gives rise to a thermal boundary resistance (TBR). Figure 1 shows the temperature profiles obtained by using the NH thermostat for various thermostat lengths L_c. For instance, in case of L_c =0.01L, the temperature jumps at the interfaces account for about 50% of the total temperature difference applied at both ends. The TBR appears due to the mismatching of the lattice-vibrational spectra of temperature controlled part and the rest of the nanotube. The mismatching gives rise to the reflection of phonons which leads to various scattering dynamics. Since TBR was found to cause variation in λ, presumably by altering the non-equilibrium local phonon distribution, the parameters L_c and relaxation time τ of the NH thermostats needed to be carefully tuned to minimize the TBR effects.

It is important to state that the above mentioned TBR effects are not entirely a numerical artifact. In the practical use of SWNTs as promoters of heat transfer, SWNTs would be bounded with connections to other materials. In this case, the heat conduction would be inevitably altered by TBRs at the connections. Therefore, in fact, it would be more realistic to examine the heat conduction of SWNTs with presence of such interfacial thermal resistance, though formulation of a general case would be difficult since such effects would be strongly case-dependent. In the current study, however, for the sake of comparison with other reported theoretical works and to focus on studying the intrinsic dynamics, we aim to construct an ideal case with minimum influence of TBRs.

3.2 Length effect of SWNT thermal conductivity

In Figure 2, thermal conductivity with phantom technique (λ_P) and Nose-Hoover (λ_{NH}) thermostats are marked with asterisks and circles, respectively. Parameters of NH thermostats were set as L_c=0.5L and τ=40ps which gives sufficiently small TBRs. Despite the difference in temperature control techniques, λ_p and λ_{NH} exhibit only minor difference within the examined range of L. This makes the phantom technique a superior method as it costs considerably less atoms than using NH thermostats. There is a relatively large discrepancy at around L~ 1 μm accompanied with the kink in the λ_p profile. We suspect this may be due the influence of thermal contraction since the nanotube length is not relaxed in case of the phantom technique while it is relaxed in case of NH thermostats. Details of the influence of thermal contraction will be reported elsewhere.

Now, let us study the general trend of the length dependence of SWNT thermal conductivity denoted with the solid line for eye. At the upper bound of L (=3.2 μm), λ takes a value around 900 W/m K. The positive gradient at the upper bound indicates that the limit of the ballistic phonon transport exceeds 3.2 μm.

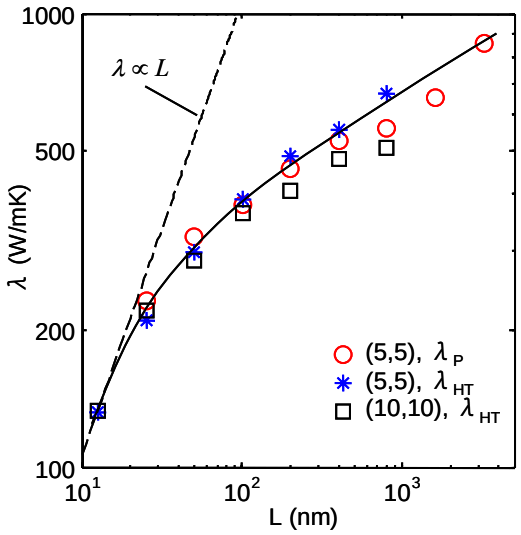

Figure 2 Length and diameter dependence of thermal conductivity of SWNTs with different temperature control methods. λ_P and λ_{NH} are the SWNT thermal conductivity calculated based on the phantom and Nose-Hoover thermostats, respectively. The solid line is drawn for eye to highlight the overall trend of the data. The dotted line denotes the length effect at the limit of pure ballistic phonon transport.

The overall trend of $\partial\lambda / \partial L$ clearly indicates the gradual transition from pure ballistic to diffusive-ballistic phonon transport. When all the phonons experience ballistic phonon transport, λ is proportional to L (constant thermal conductance). The asymptotic match of the data to $\lambda \propto L$ (dashed line) suggests the pure ballistic transport. Note, on considering the significant phonon population in the a wide range of phonon branches at room temperature, we expect contributions on the heat conduction not only from ballistic transport of acoustic phonon modes but also from that of various optical phonon modes in small L regime. This is consistent with the results of MD realization of Non-Fourier heat conduction in a nanometers long SWNT, where the ballistic transport of collective optical phonons was observed to play an important role [19]. The gradient $\partial\lambda / \partial L$ decreases as L increases, since phonons mean free paths become shorter relatively to L hence short range ballistic phonons become diffusive. In the diffusive-ballistic phonon transport regime (L > 100 nm), λ_{NH} exhibits power-law dependence on L with the exponent of approximately 0.25.

3.2 Diameter effect of SWNT thermal conductivity

Let us now examine the diameter (d) dependence of SWNT thermal conductivity. The diameter dependence reflects the weight contribution from acoustic phonons and the rest of optical phonons. Considering that a wide range of phonon branches are populated at room temperature, if the heat conduction is dominated by the ballistic transport of only acoustic phonons, λ would decrease as the diameter increases since the phonon population per branch is reduced. On the contrary, comparing λ_{NH} of (5, 5) SWNTs (asterisks) and (10, 10) SWNTs (squares), λ_{NH} is diameter-independent in L<100 nm. This means that the thermal conductance increases with A i.e. d^2, which indicates the two-dimensional nature of the heat conduction. The deviation of λ_{NH} for (10, 10) SWNTs from the ones for (5, 5) SWNTs beyond L=100 nm implies the growing relative contribution of certain selected phonons, presumably the phonons with low circumferential wave number such as the acoustic phonons. The observed diameter dependence of the length effect is consistent with the earlier discussion that the active heat carriers change from ballistic phonons of diverse branches to those with a narrower distribution.

4. Conclusions

Non-equilibrium MD simulations were conducted to investigate the SWNT heat conduction in terms of phonon transport. Imposition of a temperature gradient on an SWNT using thermostats typically gives rise to thermal resistances at the boundaries between temperature-controlled layers and the rest of the nanotube, which alter the heat conduction characteristics. By tuning the thermostats to minimize the thermal boundary effect, the length-effect of the thermal conductivity was quantified in a range of L up to 3.2 μm. The gradual transition from nearly pure ballistic phonon transport to diffusive-ballistic phonon transport was clearly observed. The positive slope at the upper bound of L indicates that the limit of ballistic phonon transport exceeds 3.2 μm. In the small L regime with strong ballistic transport, there is a significant contribution on the heat conduction from a wide range of optical phonons at room temperature. Corresponding picture was obtained from the diameter dependence where λ is L-invariant when L<100 nm. The current simulation results imply that, one needs to take the ballistic transport of diverse phonon branches into account on computing λ of short SWNTs at room temperature.

REFERENCES

[1] Saito, R., Dresselhaus, G. and Dresselhaus, M. S., Physical Properties of Carbon Nanotubes, Imperial College Press, London (1998).
[2] Berber, S., Kwon, Y-K. and Tomanek, D., Phys. Rev. Lett. 84 (2000), 4613.
[3] Yu, C., Shi, L., Yao, Z., Li, D. and Majumdar, A., Nano Lett. 5 (2006), 1842.
[4] Pop, E., Mann, D., Wang, Q., Goodson, K. and Dai H., 6 (2006), 96.
[5] Kim, P., Shi, L., Majumdar, A. and McEuen, P. L., Phys. Rev. Lett. 87 (2001), 215502.
[6] Fujii, M., Zhang, X., Xie, H., Ago, H., Takahashi, K., Ikuta, T., Abe H. and Shimizu, T., Phys. Rev. Lett. 95 (2005), 065502.
[7] Chen, G.., Nanoscale Energy Transport and Conversion, Oxford University Press, New York (2005).
[8] Maruyama, S., Physica B, 323 (2002), 272.
[9] Maruyama, S., Micro. Therm. Eng., 7 (2003), 41.
[10] Livi, R. and Lepri, S., Nature, 421 (2003), 327.
[11] Mingo, N. and Broido, D. A., Nano Lett. 5 (2005), 1221.
[12] Wang, J. and Wang, J-S., Appl. Phys. Lett. 88 (2006), 111909.
[13] Brenner, D. W., Phys. Rev. B, 42 (1990), 9458.
[14] Yamaguchi, Y. and Maruyama, S., Chem. Phys. Lett., 286 (1998), 336.
[15] Hone, J., Whitney, M., Piskoti, C. and Zettl, A., Phys. Rev. B. 59 (1999), R2514.
[16] Yamamoto, T., Watanabe, S. and Watanabe, K., Phys. Rev. Lett. 92 (2004), 075502.
[17] Nose, S., J. Chem. Phys., 81 (1984), 511.
[18] Hoover, W. G., Phys. Rev. A, 31 (1985), 1695.
[19] Shiomi, J. and Maruyama, S., Phys. Rev. B 73 (2006), 205420.